RevMexAA (Serie de Conferencias), **15**, 172–174 (2003)

COMETARY COMPACT H II REGIONS

M. G. Hoare, S. L. Lumsden, A. L. Busfield, and P. Buckley

Department of Physics and Astronomy, University of Leeds, UK

RESUMEN

Presentamos las estructuras de velocidad del gas molecular e ionizado de cuatro regiones H II compactas cometarias. Los gradientes de la velocidad en las colas de las estructuras cometarias apoyan la idea de un flujo de "champán" y no son consistentes con la interpretación de un choque de proa. Una estructura de velocidad significativa en la cabeza requiere de componentes dinámicos adicionales, los cuales pudieran deberse a la influencia de los vientos estelares.

ABSTRACT

We present velocity structures in the ionized and molecular gas of four cometary compact H II regions. Velocity gradients in the tails of the cometary structures support a champagne flow and are inconsistent with a bow-shock interpretation. Significant velocity structure at the head requires additional dynamical components, which may well arise from the influence of stellar winds.

Key Words: **H II REGIONS**

1. INTRODUCTION

H II regions play an important role in many aspects of star formation, apart from being an obvious manifestation of new massive stars. Their expansion could trigger further molecular clumps to collapse in a sequential star-formation scenario (Elmegreen & Lada 1977) by increasing the external pressure or by radiatively driven implosion (e.g., Lefloch & Lazareff 1994). Conversely, this expansion will also help to disperse the molecular cloud, eventually causing the end of the star-formation episode and partly determining the star-formation efficiency (Franco, Shore, & Tenorio-Tagle 1994). Before these competing effects can be addressed, a firm understanding of the dynamical evolution of H II regions is required.

A renaissance in the study H II region dynamics was triggered by high-resolution radio studies of a large sample of ultra-compact H II regions (UCHIIs) by Wood & Churchwell (1989). They found these objects in large numbers and with a preponderance of cometary morphologies. New dynamical models were developed to address both aspects. A bowshock model was proposed in which the stellar wind from a moving OB star interacts with the molecular cloud (Mac Low et al. 1991). The geometry of such an interaction had been worked out by Dyson (1975). Redman, Williams, & Dyson (1998) invoked a mass-loading scenario giving rise to a recombination front rather than an ionization front. An asymmetric distribution of mass-loading centers then causes a cometary appearance. The idea of a massive star forming away from the center of a molecular cloud, such that the H II region expands into an asymmetric density distribution and so becomes cometary, had been originally suggested by Israel (1978). Yorke, Tenorio-Tagle, & Bodenheimer (1983) developed this into a dynamical model where once the ionization front reaches the edge of the cloud a "champagne flow" develops.

We can distinguish between the bowshock, recombination front and champagne flow models for cometary, compact H II regions by examining the velocity structure within the ionized gas and how it relates to the surrounding molecular gas. Wood & Churchwell (1991) used radio recombination lines in the archetypal cometary G 29.96−0.02 and concluded that it was consistent with the bowshock model. However, other radio studies also found evidence for champagne flows (e.g., Garay, Lizano, & Gómez 1994). Radio recombination lines are relatively weak, which means there is a trade-off between spatial resolution and sensitivity. We have taken a different approach using the much stronger near-IR recombination lines. Our first study of G 29.96−0.02 concluded that there is definite evidence of streaming motion in the tail of the cometary object, consistent with a champagne flow (Lumsden & Hoare 1996, 1999). The velocity structure at the head was also very strong and not easily explainable by any one of the models without modification. Here we present initial results from the rest of that observational campaign.

2. OBSERVATIONS

The long-slit spectra were taken with the CGS4 echelle spectrograph on UKIRT at a velocity resolution of $18\,\mathrm{km\,s^{-1}}$. The slit was aligned with the axis of the cometary region and was stepped across the

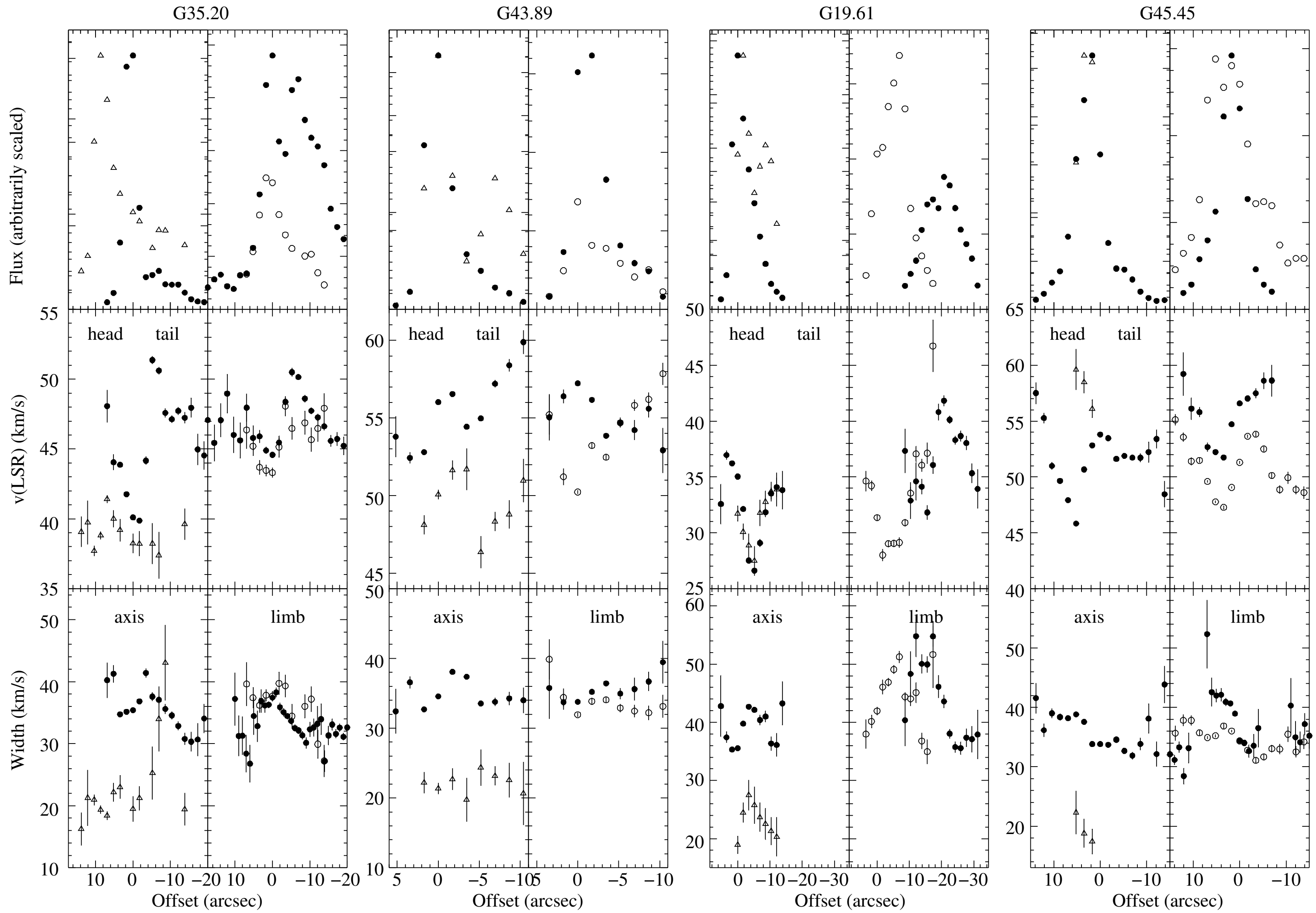

Fig. 1: Velocity structures for the four cometary regions (left to right) G 35.20, G 43.89, G 19.61, and G 45.45. The panels show the trend of the Brγ line flux (top), velocity centroid (middle) and FWHM (bottom) along the slit from the head to the tail of the cometary structure. The lefthand panel for each object shows the structure on the axis whilst the righthand one shows the stucture at each limb (open and closed circles). The limb is taken to be $4''$, $2''$, $4''$, and $2''$ from the axis, respectively, for the four regions. The on-axis velocity structure in molecular hydrogen is shown by the open triangles.

object to map velocity structure in the ionized gas using the Brγ line. An on-axis spectrum of the H_2 1–0 line was obtained to probe the velocity structure in the molecular gas immediately surrounding the nebulae. Details of the calibration procedure can be found in Lumsden & Hoare (1996, 1999).

3. RESULTS

Figure 1 presents the results for four cometary compact H II regions selected on the basis of the their radio morphology from Wood & Churchwell (1989). For G 35.20 on the axis we see firstly redshifted ($48\,\mathrm{km\,s^{-1}}$) emission at the very front of the head, which becomes relatively blue ($40\,\mathrm{km\,s^{-1}}$) just behind the peak flux and then switches back to red ($51\,\mathrm{km\,s^{-1}}$) again in the tail. This red-blue-red structure has a very similar shape and magnitude, but is opposite in direction to the blue-red-blue structure seen in G 29.96. We account for this by changing the viewing angle such that the tail of G 35.20 is pointing away from us, whereas in G 29.96 it is pointing towards us. The strong blue-to-red gradient in the tail persists at the limbs of G 35.20, which is again strong evidence for champagne flows in the tail, whereas the bowshock model predicts little velocity structure at the limbs. Once again, all the line profiles were well fitted by a single Gaussian with no evidence for two peaks as predicted by the recombination front models of Redman et al. (1998). The strong switch to blue again in the head region of G 35.20 is hard to explain in a simple champagne flow as was found for G 29.96. There is some evidence of enhanced line widths at the head as there were for G 29.96, which again are difficult to account for in any of the models.

G 43.89 is more difficult to fit into the picture outlined above. There is a strong shift to the red in the tail on-axis and in one of the limb positions, implying a champagne flow away from us. However, there is a small blue-red-blue structure around the flux peak, which would argue for the opposite orientation. The line widths are enhanced around this region so it is possible that another dynamical component, e.g., wind interacting with the inner nebula, is adding to the complexity. G 19.61 shows a very strong red-blue-red structure similar to G 35.20 on-axis and also shows streaming motions to the red on the limbs in the tail consistent with a champagne flow away from us. The off-axis structure is very asymmetric here, probably because the slits we used have a PA of 90° when 120° would be more appropriate. Across the brightest part of the axis of G 45.45 there is a switch from blue ($45\,\mathrm{km\,s^{-1}}$) to red ($54\,\mathrm{km\,s^{-1}}$) and back towards blue again ($52\,\mathrm{km\,s^{-1}}$), suggesting a similar picture to G 29.96. However, there is a very strong shift to red in the faint regions ahead of the apex and like G 43.89 this does not fit into any simple picture.

The molecular gas velocities in G 35.20 and G 43.89 are relatively constant across the structure. The ionized gas velocities are all more redshifted, which would be consistent with most of the H II region streaming away from the molecular cloud as implied by the gradient of Brγ in the tail. In G 19.61 the H_2 has very strong velocity structure that follows very closely that in the ionized gas. This emission must arise from a region that is very close to the ionization front, within the thin, shocked zone around the ionization front.

4. CONCLUSIONS

In most of these compact cometary H II regions we are seeing streaming motions in the tail consistent with the champagne flow model. At the head, and sometimes around the position of the exciting star, there are strong motions that are not explained by a simple champagne flow. New dynamical models of champagne flows which use realistic density gradients and include the effects of stellar winds are needed. Preliminary calculations of these and their direct confrontation with data are promising (Priestley 1999). Near-IR integral field spectroscopy would help to determine the relationship of the molecular hydrogen emission to the ionized gas and its excitation mechanism.

REFERENCES

Dyson, J. E. 1975, Ap&SS, 35, 299
Elmegreen, B. G., & Lada C. 1977, ApJ, 214, 725
Franco, J., Shore, S. N., & Tenorio-Tagle G. 1994, ApJ, 436, 795
Garay, G., Lizano, S., & Gómez Y. 1994, ApJ, 429, 268
Israel, F. P. 1978, A&A, 90, 769
Lefloch, B., & Lazareff, B. 1994, A&A, 289, 559
Lumsden, S. L., & Hoare, M. G. 1996, ApJ, 464, 272
——————. 1999, MNRAS, 305, 701
Mac Low, M.-M., Van Buren, D., Wood, D. O. S., & Churchwell, E. 1991, ApJ, 369, 395
Priestley, C. 1999, Ph.D. thesis, University of Leeds
Redman, M. P., Williams, R. J., & Dyson, J. E. 1998, MNRAS, 298, 33
Wood, D. O. S., & Churchwell, E. 1989, ApJS, 69, 831
——————. 1991, ApJ, 372, 199
Yorke, H. W., Tenorio-Tagle, G., & Bodenheimer, P. 1983, A&A, 127, 313

P. Buckley, A. L. Busfield, M. G. Hoare, and S. L. Lumsden: Department of Physics and Astronomy, University of Leeds, Leeds, LS2 9JT, UK (pb,alb,mgh,sll@ast.leeds.ac.uk).